EUMETSAT Satellite Application Facility on Climate Monitoring

Algorithm Theoretical Baseline Document

Meteosat Solar Surface Radiation and effective Cloud Albedo Climate Data Records - Heliosat

SARAH

The MAGICSOL method applied for the generation of SARAH

doi: 10.5676/EUM_SAF_CM/SARAH/V001

Effective Cloud Albedo (CAL)	**CM-23081**
Surface Incoming Shortwave Radiation (SIS):	**CM-23201**
Direct Normal Irradiance (DNI):	**CM-23231**

Document Signature Table

	Name	Function	Signature	Date
Author	Richard Müller Jörg Trentmann	CM SAF scientist		01/11/2014
Editor	Jörg Trentmann	DRR Coordinator		01/11/2014
Approval	Rainer Hollmann	CM SAF Science Coordinator		01/11/2014
Release	Martin Werscheck	Project Manager		

Distribution List

Internal Distribution	
Name	No. Copies
DWD Archive	1
CM SAF Team	1

External Distribution		
Company	Name	No. Copies
PUBLIC		1

Document Change Record

Issue/ Revision	Date	DCN No.	Changed Pages/Paragraphs
1.0	01/09/2013	SAF/CM/DWD/ATBD/METEOSAT_HEL	First official version.
1.1	02/12/2013	SAF/CM/DWD/ATBD/METEOSAT_HEL	Review Comments included
1.2	08/08/2014	SAF/CM/DWD/ATBD/METEOSAT_HEL	Added/modified paragraph 4.4 about the used aerosol information
1.3	01/11/2014	SAF/CM/DWD/ATBD/METEOSAT_HEL	Modifications according DRR2.1 review comments.

Applicable Documents

Reference	Title	Code
AD 1	CM SAF Product Requirements Document	SAF/CM/DWD/PRD/2.4
AD 2	Requirements Review Document	SAF/CM/DWD/RR/21

Reference Documents

Reference	Title	Code
RD.1	Algorithm Theoretical Baseline Document, Meteosat (MVIRI) Solar Irradiance and effective Cloud Albedo Climate Data Sets, MVIRI_HEL; The MAGICSOL method	SAF/CM/DWD/ATBD/MVIRI_HEL/1.3

Table of Contents

List of Figures

List of Tables

1 The EUMETSAT SAF on Climate Monitoring (CM SAF)

The importance of climate monitoring with satellites was recognized in 2000 by EUMETSAT Member States when they amended the EUMETSAT Convention to affirm that the EUMETSAT mandate is also to "contribute to the operational monitoring of the climate and the detection of global climatic changes". Following this, EUMETSAT established within its Satellite Application Facility (SAF) network a dedicated centre, the SAF on Climate Monitoring (CM SAF, http://www.cmsaf.eu).

The consortium of CM SAF currently comprises the Deutscher Wetterdienst (DWD) as host institute, and the partners from the Royal Meteorological Institute of Belgium (RMIB), the Finnish Meteorological Institute (FMI), the Royal Meteorological Institute of the Netherlands (KNMI), the Swedish Meteorological and Hydrological Institute (SMHI), the Meteorological Service of Switzerland (MeteoSwiss), and the Meteorological Service of the United Kingdom (UK MetOffice). Since the beginning in 1999, the EUMETSAT Satellite Application Facility on Climate Monitoring (CM SAF) has developed and will continue to develop capabilities for a sustained generation and provision of Climate Data Records (CDRs) derived from operational meteorological satellites.

In particular the generation of long-term data records is pursued. The ultimate aim is to make the resulting data records suitable for the analysis of climate variability and potentially the detection of climate trends. CM SAF works in close collaboration with the EUMETSAT Central Facility and liaises with other satellite operators to advance the availability, quality and usability of Fundamental Climate Data Records (FCDRs) as defined by the Global Climate Observing System (GCOS). As a major task the CM SAF utilizes FCDRs to produce records of Essential Climate Variables (ECVs) as defined by GCOS. Thematically, the focus of CM SAF is on ECVs associated with the global energy and water cycle.

Another essential task of CM SAF is to produce data records that can serve applications related to the new Global Framework of Climate Services initiated by the WMO World Climate Conference-3 in 2009. CM SAF is supporting climate services at National Meteorological and Hydrological Services (NMHSs) with long-term data records but also with data records produced close to real time that can be used to prepare monthly / annual updates of the state of the climate. Both types of products together allow for a consistent description of mean values, anomalies, variability and potential trends for the chosen ECVs. CM SAF ECV data records also serve the improvement of climate models both at global and regional scale.

As an essential partner in the related international frameworks the CM SAF assumes the role as main implementer of EUMETSAT's commitments in support to global climate monitoring. This is achieved through:

- Application of highest standards and guidelines as lined out by GCOS for the satellite data processing,
- Processing of satellite data within an international collaboration benefiting from developments at international level and pollinating the partnership with own ideas and standards,
- Intensive validation and improvement of the CM SAF climate data records,
- Taking a major role in data record assessments performed by research organisations such as WCRP (World Climate Research Programme),
- Maintaining and providing an operational and sustained infrastructure that can serve the community within the transition of mature CDR products from the research community into operational environments.

A catalogue of all available CM SAF products is accessible via the CM SAF webpage, www.cmsaf.eu. Here, detailed information about product ordering, add-on tools, sample programs and documentation is provided.

2   Introduction

For climate monitoring and climate analysis time series of climate variables of sufficient length (i. e., spanning multiple decades) are required. To generate such long time series, the satellite information of the first generation of Meteosat satellites (Meteosat-2 to Meteosat-7, covering 1982 to 2005) has to be employed. The MVIRI instrument on-board the Meteosat First Generation satellites is equipped with three channels: a broadband channel in the visible, a channel in the infrared, and a water vapor channel.

The second generation of Meteosat satellites (Meteosat-8 to (currently) Meteosat-10, covering 2005 to today) is equipped with the Spinning Enhanced Visible and Infrared Imager (SEVIRI) and the Geostationary Earth Radiation Budget (GERB) instrument. The GERB instrument is a visible-infrared radiometer for earth radiation budget studies. It provides accurate measurements of the shortwave (SW) and longwave (LW) components of the radiation at the top of the atmosphere. SEVIRI employs twelve spectral channels, which provide more information of the atmosphere compared to its forerunner. Several retrieval algorithms have been developed to use the additional information gained by the improved spectral information of Meteosat Second Generation (MSG) mainly for nowcasting applications. However, these algorithms can not be applied to the MVIRI instrument on-board the Meteosat First Generation (MFG) satellites as they use spectral information that is not provided by MFG (e. g., the NWC SAF cloud algorithm, the CM SAF operational radiation algorithm).

As a consequence, in order to be able to provide a long time series covering more than 20 years, a specific climate algorithm has to be applied to the satellite observations from the first and second generation of Meteosat satellites.

The MAGICSOL method is a combination of the well established Heliosat method (see section 3) with the gnu-public license version of the Mesoscale Atmospheric Global Irradiance Code (MAGIC). MAGICSOL does meet the above mentioned requirements. The method provides the effective cloud albedo, the solar surface irradiance, and the net shortwave radiation, i. e., relevant components of the GCOS Essential Climate Variables (ECVs) surface radiation budget and cloud properties.

The MAGICSOL method requires as satellite information only the measurements of the broadband visible channel and can therefore be applied across different satellite generations. The application to observations from other geostationary satellites, e.g., GOES and GMS, is also possible. Hence, the MAGICSOL method has not only the power to provide long time series of ECVs, but also to provide ECVs, which cover the complete geostationary ring.

The basis of the cloud part of the MAGICSOL method is the Heliosat method, which is well established in the solar energy community. However, modifications of the original Heliosat method were needed to meet the requirements to generate a Climate Data Record. This modification is discussed in section 3.3.

In comparison to the method and input data used for the generation of the first MVIRI only climate data record of the CM SAF (RD.1) the following things have been modified.

On the one hand the method for the retrieval of the clear sky reflection has been modified. The method applied for the generation of the current data record is discussed in section 3.4. This modification was needed because the former approach (Fuzzy logic approach, see RD.1) led to artefacts in the effective cloud albedo. Additionally a bug in the routine for the calculation of the scanning time of the pixels has been fixed.

Further, a new aerosol climatology has been used. This climatology reduces the uncertainty of the data record (Mueller and Träger-Chatterjee, 2014) and is discussed in section 4.4. Finally, the image data of MFG have been visually inspected (1983-1994). Corrupt images

have been either corrected or have been not used for the processing of the climate data record. This is further discussed in section 3.5. The modifications relative to RD.1 are summarized in section 6.The generated 31 year long (1983-2013) continuous surface radiation climate data record is based on observations from the Meteosat First and Second Generation satellites and is called SARAH: Surface Solar Radiation Data record – Heliosat.

Table 2-1: Overview of Meteosat based data records discussed in this ATBD.

Acronym	Product title	Unit
SIS	Surface Incoming Shortwave Irradiance	W/m^2
CAL	Effective Cloud Albedo	Dimensionless
DNI	Direct Normal Irradiance at surface	W/m^2

3 The Heliosat method

3.1 The original Heliosat algorithm

The Heliosat algorithm uses reflection measurements given as normalized digital counts to determine the effective cloud albedo, also called cloud index (Cano et al., 1986; Beyer et al., 1996; Hammer et al., 2003). A clear sky model is used afterwards to calculate the solar surface irradiance based on the retrieved effective cloud albedo. Basis of the Heliosat method are the digital counts of the visible Meteosat channel. No information from NIR or IR channels is required.

The first step in the Heliosat method is the retrieval of the effective cloud albedo (cloud index), n, i. e. the normalised relation between the all sky and the clear sky reflection in the visible channel observed by the satellite:

$$n = \frac{\rho - \rho_{srf}}{\rho_{max} - \rho_{srf}}$$

(Equation 3-1)

Here, ρ is the observed reflection for each pixel and time. ρ_{sfc} is the clear sky reflection, and ρ_{max} is an estimate for the maximum reflectivity observed by the satellite. Further details on the calculation of the effective cloud albedo can be found in RD.1, Section 3.1.

3.2 From Heliosat to MAGICSOL

To meet the requirements of a CDR some modifications of the original Heliosat algorithm have been performed, resulting in a version of the Heliosat algorithm for the generation of climate data records. In particular a self-calibration algorithm (see section 3.3), which dynamically accounts for changes in sensor sensitivity, has been developed. The modified version of the Heliosat algorithm in combination with the gnu-MAGIC approach (see section 4) is called MAGICSOL.

The MAGICSOL approach has been used in the processing of the CM SAF surface radiation data record based on the MVIRI instruments on-board the first generation of Meteosat satellites (Posselt et al., 2012). Full details of the algorithm are presented in RD.1 and Posselt et al., 2012. In comparison to the version discussed in RD.1 two modifications have been performed, which are discussed in section 3.4. Here we provide an overview of the method and present the adjustments required to process the data from the second generation of Meteosat satellites.

3.3 Self calibration

The self-calibration algorithm is based on an operational and automatic determination of the maximum reflectivity ρ_{max}. In analogy to Rigollier et al. (2002) a histogram of all available

counts is generated and the 95th-percentile is used as self-calibration parameter and set to ρ_{max} (Hammer et al., 2003 and references therein). Only satellite pixels located in the southern Atlantic between 15° W and 0° W and 58° S and 48° S are considered. This region features a high abundance of frontal systems with large cloud amounts most of the time, but hardly any convection. The statistical analysis is based on one month of satellite data at 13 UTC. The resulting estimate for ρ_{max} is then applied to all slots within that month.

Further details and a validation of the self calibration method can be found in Posselt et al., 2012 and RD.1.

3.4 Clear sky reflection

The processing of the long time series of surface solar radiation from the geostationary Meteosat satellites employs a robust clear sky or background reflection method based on Hammer, 2000. This method replaces the method of Dürr and Zelenka (2009), which was used in the processing of the CM SAF MVIRI-based surface radiation data record (Posselt et al., 2012). While the previously used method works well over snow covered regions, it has some weakness over desert regions.

The clear sky reflection is derived from the frequency distribution of the observed reflections during an appropriate time period. This frequency distribution exhibits one peak for cloudy and a separate peak for clear sky reflection. The peak for clear sky reflection is usually significantly lower and at the lower end of the overall frequency distribution, the dark counts. Thus, the clear sky reflection can be estimated by a minima approach. Using the lowest value of the reflection within a certain time period might be an option. However, the lowest values are often a result of cloud shadows and therefore do not represent the clear sky reflection. Hence, the clear sky reflection can be interpreted as a stationary variate with a mean value ρ_{sfc} and a variance ε. All values above a starting value ρ_{sfc} plus the ε are iteratively sorted out. After each iteration step a new mean is derived, accordingly a new limit for the sorting applies.

The iteration process is given in Equation 3-1. The calculated mean iterates to the clear sky reflection ρ_{sfc} if Equation 3-2 is valid. Here ρ_{cld} and ε_{cld} are the respective values for clouds.

$$\text{starting value}: \ \rho_{srf} = \max(datarange)$$
$$\text{iteration}: \text{if} \left(\rho < \rho_{srf} + \varepsilon\right) \rightarrow \rho_{srf} = \rho$$
$$\text{(change)} \hspace{3cm} \textbf{(Equation 3-1)}$$
$$\text{else}: \rightarrow \rho_{srf} = \rho_{srf}$$
$$\text{(no change)}$$

$$\rho_{cld} - \rho_{srf} > \max(\varepsilon, \varepsilon_{cld}) \hspace{2cm} \textbf{(Equation 3-2)}$$

The clear sky reflection is derived for every pixel and every slot. The time series has to be long enough to contain cloudless conditions for every pixel. However, the time series should be also short enough to consider seasonal changes in the surface albedo. Hence, a time span of about 1 month is assumed to be appropriate and widely used. The surface albedo exhibits a strong dependency on the solar zenith angle. The surface albedo in turn is the driving factor for the clear sky reflection. Hence, the method is applied for every slot, in order to resolve the solar zenith angle dependency. As the mean of the dark counts is used values of CAL below of 0 might occur.

3.5 Input data

From the MVIRI instruments on-board the first generation of Meteosat satellites the rectified digital pixel counts of the broadband visible MVIRI channel are used. The respective data are called *"Rectified Image Data"* and provided by EUMETSAT (EUM TD 06) in openMTP format. However, other formats and satellite images can be treated as well. Rectified images containing counts are used.

The SEVIRI instruments on-board the second generation of Meteosat satellites do not continue to provide the same spectral broadband information as the MVIRI instruments. For a consistent prolongation of the time series from the MVIRI instruments broadband observations have to be used (Posselt et al., 2011). A linear combination of the MSG/SEVIRI visible narrowband channels (VIS006 and VIS008) will be used (Cros et al., 2006, see Figure 3-1). This approach has been proven to enable a homogenous retrieval of surface solar radiation between MFG and MSG (Posselt et al., 2013). For comparison purposes also the broadband top of atmosphere albedo retrieved from GERB/SEVIRI by RMIB will be used.
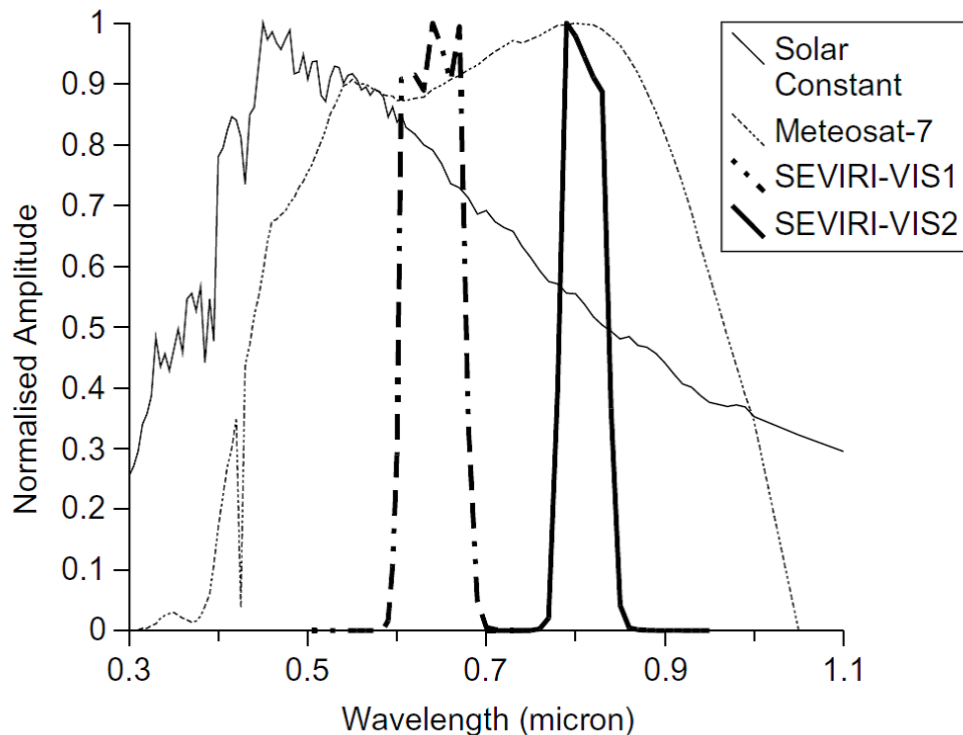
Figure 3-1: Normalized spectral responses for the broadband visible channel of MVIRI and the two visible bands of SEVIRI. Also shown is the normalized solar spectral irradiance (Figure taken from Cros et al., 2006).

The first MVIRI climate data record of CM SAF shows stripe artefacts in the radiation products, e.g. see Figure 3-2 for example. It has been evaluated that these stripes are due to stripes in the MVIRI raw images, see Figure 3-3 (left hand) for example.
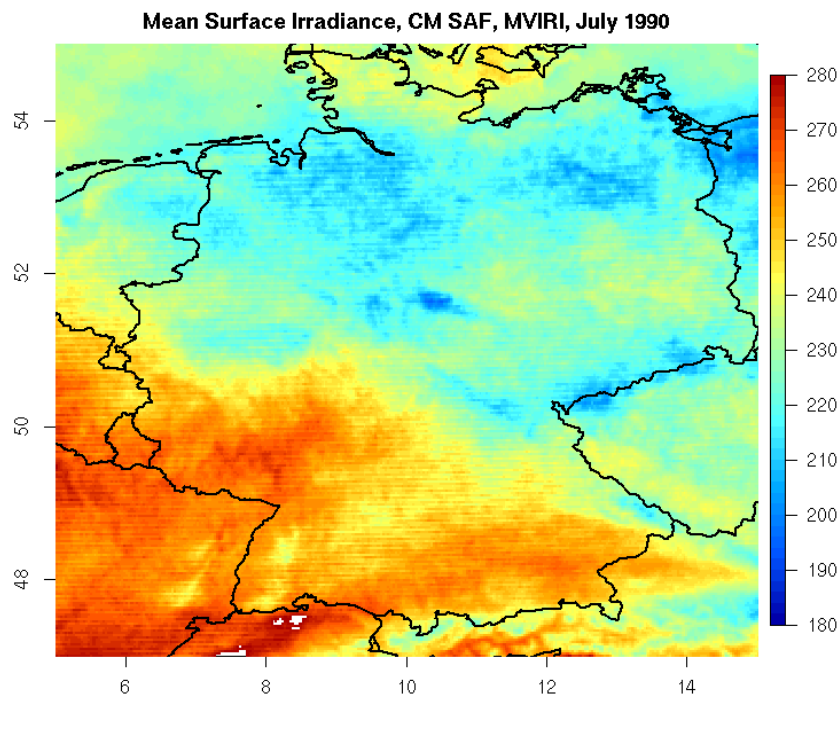
Figure 3-2: Example of striped CM SAF radiation product of the first MVIRI climate data record in W/m^2.

Therefore all MVIRI raw images covering the time period 1983-1994 have been visually inspected. It has been found that a lot of raw images of Meteosat First Generation show so far undocumented stripes. For those images only every second line is defined. This led to stripes in the radiation products as well (see CM SAF service messages and Figure 3-2 for example). The missing lines have been filled by spatial-temporal interpolation in order to have enough images for the processing and to gain the optimal information content out of the images, see for example Figure 3-3. Images with unfixable bugs have been identified and have not been used for the processing.
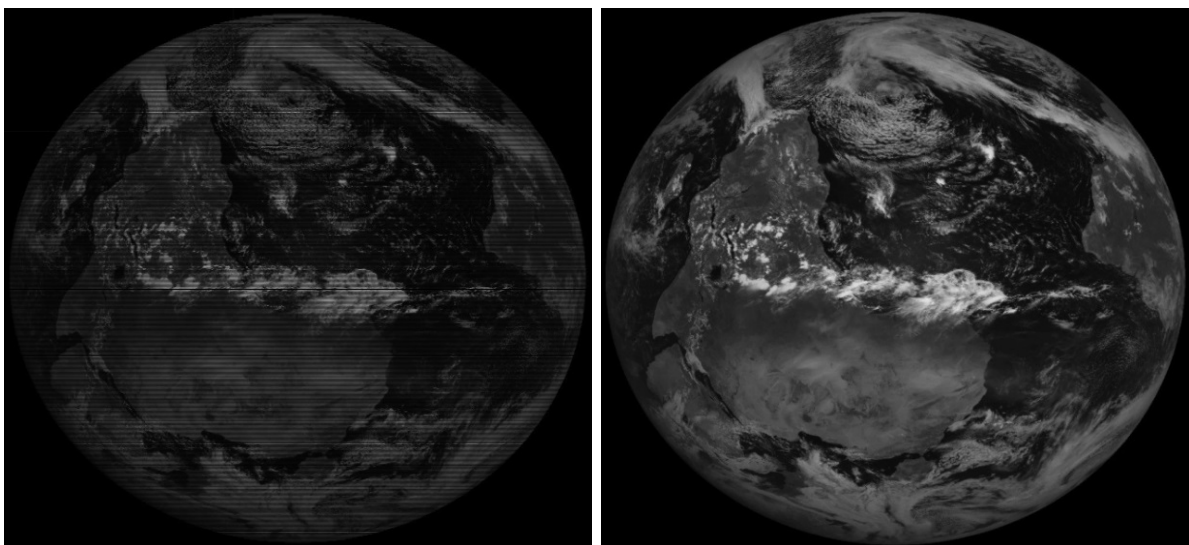
Figure 3-3: Left hand raw image of Meteosat First Generation with stripes, right hand, respective image without stripes after succesful correction.

11

3.6 Effective cloud albedo (CAL)

The effective cloud albedo is derived with the MAGICSOL method described in Section 3.2. Clouds have a net cooling effect, which is several magnitudes higher than the forcing caused by the increase of greenhouse gases. Every trend and anomalies in the effective cloud albedo would significantly affect the climate system on a global and/or regional scale. The effective cloud albedo is therefore an essential climate variable although not explicitly defined as such by GCOS. As clouds can be assumed as Lambertian surfaces, the derived quantity can be considered the effective cloud albedo.

3.6.1 Averaging

Monthly, daily and hourly means are calculated by arithmetic averaging, using Equation 3-3.

$$CAL_{mean} = \frac{\sum_{i=1}^{n} CAL_i}{n}$$ **(Equation 3-3)**

Here is either a loop over the slots per hour for the calculation of hourly means, or a loop over the hourly means for the calculation of the daily means, or a loop over daily means for the calculation of monthly means. Only the finite values of CAL are taken into account, n is the total number of finite values

The hourly means are derived from 3 observational slots, e. g., 1200 is the average of the 12:00, the 12:30 and the 13:00 slot (all times are the start time of the scan). This guarantees a higher stability in the hourly means in case of missing slots. To ensure consistent averaging and prevent double counting each full hour slot is weighted only with 25 % in the averaging (i. e., CALhm (1200) = 0.25 CAL(1200) + 0.5 CAL(1230) + 0.25 CAL(1300)).

A minimum number of three available hourly means per day is required to derive the daily mean for this specific pixel. The monthly average is calculated from the daily means of this month for each pixel as the arithmetic mean with a required number of 10 existing daily means.

The conversion from the irregular satellite projection to the regular 0.05 x 0.05 degree lon-lat-grid is conducted with the gnu-MAGIC gridding tool based on a nearest-neighbour method.

3.7 Uncertainty of the cloud albedo retrieval

The uncertainty associated with the retrieval of the effective cloud albedo can be estimated based on the sensitivty of CAL on the paramters used in the retrieval of CAL. Here we summarize the main results of the sensitivity assessment, details can be found in RD.1.

3.7.1 Sensitivity of the effective cloud albedo on ρ_{max} and ρ_{srf}

The effective cloud albedo is defined as a relative quantity of observed counts or radiances. Hence, any noise or uncertainty in the satellite observations is predominantly cancelled out. The uncertainty in the effective cloud albedo is therefore pre-dominantly determined by uncertainties in the determination of the clear sky reflection and the self-calibration method.

3.7.2 Sensitivity of CAL on self-calibration method

The uncertainty or fuzziness in ρ_{max} defined by the month to month variations of ρ_{max} is in the order of 3 %. However, it is likely that part of this uncertainty is due to the variability in the satellite counts, which will cancel out in the calculation of the effective cloud albedo (Equation 3 2), and, hence, do not affect the accuracy of CAL. Under the worst case

assumption of an uncertainty of ρ_{max} of 3 % the uncertainty of CAL is in the order of 5 % over bright surfaces. However, such high uncertainties occur only for high CAL values, hence the effect on solar irradiance is rather low. Further information can be found in RD.1.

3.7.3 Sensitivity of CAL on clear sky reflection

The impact of the uncertainty in the determination of the clear sky reflection on the effective cloud albedo is low as a consequence of the occurrence of ρ_{srf} in the dominator and nominator of the effective cloud albedo formula.

However, the clear sky reflection can introduce significant uncertainty and error in the effective cloud albedo retrieval for the case of cloud contamination. This happens if not enough clear sky cases occur. Hence, for regions with long-lasting cloud cover in combination with slant geometry the ρ_{srf} retrieval fails to see the clear sky situations, thus ρ_{srf} is contaminated by clouds and not representative for clear sky conditions. This effect occurs pre-dominantly at the border of the Meteosat disk, above 60 degrees. As it occurs only for regions with long-lasting cloud coverage (hence large values of the effective cloud albedo) the effect on the solar irradiance is much lower as implied by the uncertainty in the effective cloud albedo. Further information and graphical illustrations of these effects can be found in RD.1.

3.8 Limitations, assumptions and future improvements

Below is a list of some of known deficiencies and limitations of the algorithm to derive CAL:

- In general, the sensitivity of the MAGICSOL method to detect clouds is reduced over bright surfaces, which does lead to an under-detection of clouds over bright surfaces, e. g., desert and snow.
- The clear sky reflection, ρ_{sfc}, can accurately be retrieved if a certain number of clear sky cases are available within a month. This is not always the case.
- Snow-covered surfaces might be interpreted as clouds by the algorithms, resulting in an overestimation of the effective cloud albedo.
- The anisotropy of the cloud reflection leads to uncertainties in the effective cloud albedo and subsequent in the solar surface irradiance. The respective effect is in the order of 1 to 2 % for monthly and daily means respectively. However, in general the anisotropy effect of clouds is rather small.

3.9 Relation of effective cloud albedo to solar irradiance

The effective cloud albedo is related to the solar irradiance via the clear sky index. The clear sky index, k, is defined as

$$k = SIS / SIS_{CLS}$$

resulting in the formula for the surface irradiance:

$$SIS = k \cdot SIS_{CLS}$$

Here SIS_{CLS} is the solar irradiance for cloud free skies. For most conditions the relation between the effective cloud albedo CAL and the clear sky index is given by:

$$k = 1 - CAL$$

This relation is defined by the law of energy conservation (Dagestad, 2004). Above a CAL value of 0.8 empirical corrections are needed, described in detail in Section 5.

For the retrieval of the direct irradiance a formula of Mueller et al. (2009) is used, which describes the relation of the direct irradiance (all sky) SID to that of the clear sky direct irradiance SID_{CLS}.

$$SID = SID_{CLS}\left(k - 0.38 \cdot (1-k)\right)^{2.5}$$ **(Equation 3-4)**

where k is the clear sky index and SID_{CLS} is the direct solar irradiance for clear sky conditions. This formula is an adaptation of the Skartveit et al. (1998) diffuse model.

With the knowledge of the clear sky index and the clear sky surface radiation components (global and direct), the all sky surface solar radiation can be derived using the equations given above. The clear sky solar irradiance is calculated using an eigenvector look-up table method (see Mueller et al., 2009). It is based on radiative transfer modelling and enables the use of extended information about the atmospheric state. Further details of the clear sky atmospheric radiative transfer model are presented in Section 4.

Surface solar irradiance data records derived with the Heliosat method and the n-CAL equation (Equation 5-5) have been extensively validated against the ground-based solar radiation measurements (Perez et al., 2001; Wald et al., 2002; Meyer et al., 2003; Rigollier et al., 2004, Posselt et al., 2012, Sanchez-Lorenzo et al., 2013). It is well recognized that the surface solar irradiances derived from satellite measurements have a higher accuracy than interpolated ground-based measurements, which are more than 30 km apart (Perez et al., 1998; Zelenka et al., 1999). The validation results have demonstrated that the n-CAL relation is very robust.

4 The gnu-MAGIC algorithm

The clear sky solar irradiance is calculated using an eigenvector look-up table method (see Mueller et al., 2009). It is based on radiative transfer modelling and enables the use of extended information about the atmospheric state. Accurate analysis of the interaction between the atmosphere, clear sky reflection, transmission and the top of atmosphere albedo has been the basis for this method, characterized by a combination of parameterizations and "eigenvector" look-up tables. The source code of the method (Mesoscale Atmospheric Global Irradiance Code – MAGIC) is available under gnu-public license at http://sourceforge.net/projects/gnu-magic/. A detailed description of the gnu-MAGIC algorithms can be found in RD.1 and Mueller et al., 2009.

4.1 Solar irradiance: Introduction and Definition

The solar surface irradiance consists of a diffuse fraction and a direct fraction. The diffuse fraction of the surface irradiance is defined as the solar radiation that has undergone scattering in the atmosphere. The direct irradiance is the flux reaching a horizontal unit of the earth's surface in the 0.2 – 4 µm wavelength band from the direction of the sun without being scattered. Both quantities are expressed in W/m^2.

4.2 Motivation and strategy for solar surface irradiance and direct irradiance

Accurate information on the direct and total solar irradiance is important for
- the monitoring, the analysis and the understanding of the climate system,
- the prediction of energy yield, the planning, monitoring and system design of photovoltaic systems and solar-thermal power plants
- agricultural meteorological applications.

Only few well-maintained ground measurements of irradiance (in particular, direct irradiance) exist in Europe, while in Africa and over the ocean almost no information on surface radiation is available from surface observations. Geostationary satellites enable the retrieval of area-wide total and direct irradiance in high spatial and temporal resolution with good accuracy ($<15 \ W/m^2$).

In the previous years, CM SAF has already successfully extended and applied well-established methods used within the Solar Energy community (e.g., Skartveit et al., 1998) to generate surface solar radiation data records from satellite observations. One important extension of the clear sky surface radiation algorithm (gnu-MAGIC) is the use of detailed aerosol information instead of turbidity maps. The clear sky irradiance is completely based on Radiative Transfer Modelling. Finally, the possibility to use an improved cloud mask is expected to improve the accuracy. The physical basis of the algorithm is described in Mueller et al. (2009) and Müller et al. (2003).

4.3 Algorithm Overview

In the following the gnu-MAGIC algorithm to derive the direct and total surface radiation under clear sky conditions is briefly presented. A full description can be found in RD.1 and Mueller et al., 2009.

The retrieval of the surface clear sky direct irradiance and the surface clear sky solar surface irradiance is realised using an eigenvector look-up table (LUT) approach. The LUTs for the surface direct and total solar radiation have been generated by conducting radiative transfer model (RTM) simulations using libRadtran (Mayer and Kylling, 2005) (Figure 4-1). A LUT is a data structure used to replace the time-consuming RTM computation with a simpler and faster interpolation operation within discrete pre-computed RTM results.
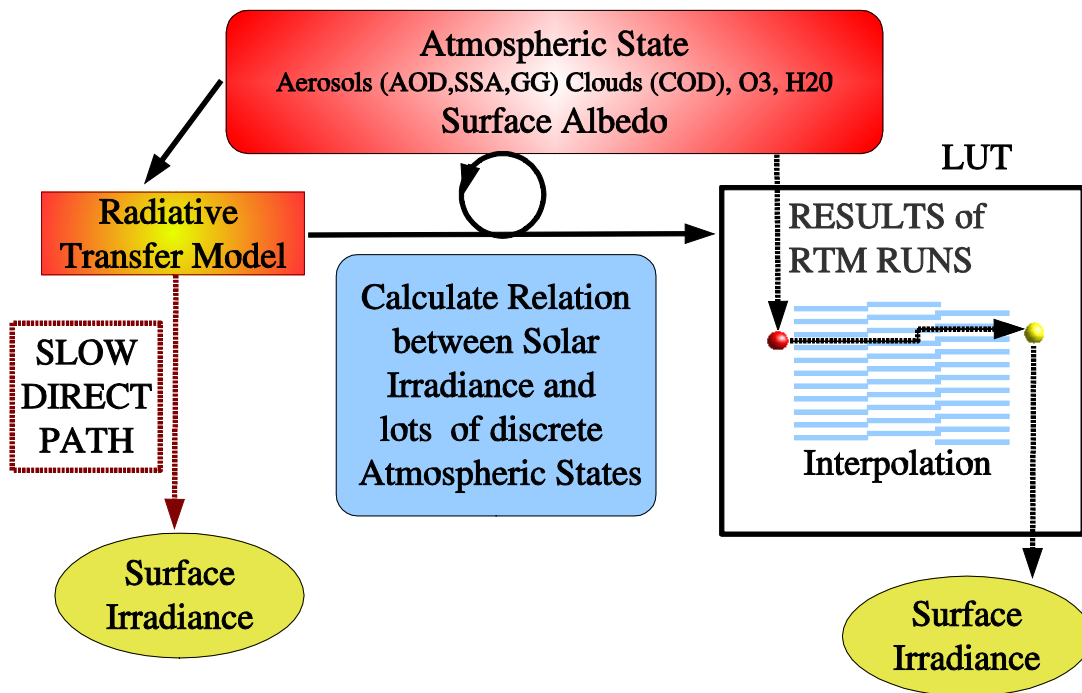
Figure 4-1: The relation of the transmission to a manifold of atmospheric states is pre-calculated with a radiative transfer model (RTM) and saved in a look-up table (LUT). Once, the LUT has been computed the transmittance for a given atmospheric state can be extracted from the LUT for each satellite pixel and time.

The clear sky LUTs consists of radiative transfer model results for aerosols with different aerosol optical thickness, single scattering albedo, and asymmetry parameter. Fixed values for water vapour, ozone and surface albedo have been used for the calculation of the basis LUT: 15 kg/m^2 for water vapour column, 345 DU of ozone, and a surface albedo of 0.2. The effect of the solar zenith angle on the transmission, hence the surface solar irradiance, is considered by the use of the Modified Lambert Beer (MLB) function (Mueller et al., 2004). The effects of water vapour and surface albedo on the surface radiation are considered using correction formulas and parameterizations. Therefore the MAGIC code is fast, robust and suitable for operational application.

The input parameters of the gnu-MAGIC code are date, time, solar zenith angle, latitude, longitude, effective cloud albedo (cloud index), water vapour column density, surface albedo, aerosol optical thickness and single scatter albedo for aerosols. The output of the gnu-MAGIC code is the total and the direct clear sky surface solar irradiance in the 0.2-4.0 µm wavelength region. The ozone column density is set to a constant value of 345 DU and the asymmetry parameter for the aerosol scattering phase function is also fixed at 0.7 in the current version of the MAGIC code. The extra terrestrial total solar irradiance is set to 1366 W/m^2 and adjusted according to the earth-sun distance. More details on the gnu-MAGIC algorithm are described by Mueller et al. (2004, 2009). For the generation of SARAH the updated spectrally resolved version of gnu-MAGIC (Mueller et al., 2012) is used.

4.4 Atmospheric input information

Here the atmospheric input information used to retrieve the clear sky surface solar irradiance is described.

Aerosol:
Aerosol particles have a significant effect on the surface solar irradiance, because they scatter and absorb solar radiation. To describe the effect of scattering and absorption, information about the aerosol type and aerosol optical depth is needed. The aerosol type determines the relation between scattering and absorption, which is expressed by the single scattering albedo. The asymmetry parameter depends also on the aerosol type (size and composition) and determines the relation between forward- and backward-scattering. For the calculation of direct irradiance only the aerosol optical depth (AOD) is relevant, as the AOD is defined as the attenuation of direct irradiance. The single scattering albedo and the asymmetry factor (both are determined by the aerosol type) are only of relevance for the total solar irradiance (diffuse + direct irradiance).
Monthly mean aerosol information is taken from an aerosol climatology by the European Centre for Medium Range Weather Forecast (ECMWF) – MACC (Monitoring Atmospheric Composition and Climate). The MACC data results from a data assimilation system for global reactive gases, aerosols and greenhouse gases. It consists of a forward model for aerosol composition and dynamics (Morcrette et al., 2009) and the data assimilation procedure described in detail in (Benedetti et al., 2009). It has recently been used for the estimation of aerosol radiative forcing (Bellouin et al., 2013). The MACC reanalysis data is generated on a Gaussian T159 grid which corresponds ~ to 120 km resolution. For the use within CM SAF it has been regridded to a 0.5x0.5 degree regular latitude longitude grid.
MACC has been evaluated to perform significantly better than Kinne et al. and GADS/OPAC climatology (Hess et al., 1998, Köpke et al. 1997), see Mueller and Träger-Chatterjee (2014) for further details.

Water vapour:
Water vapour is an important atmospheric absorber in the solar spectral range.
Monthly values of the vertically-integrated water vapour are taken from the ERA-Interim global reanalysis data record of ECMWF (Dee et al., 2011).

Ozone:
Ozone is a strong absorber in the UV spectral range, but the absorption is quite weak within the broadband spectrum, which is relevant for the estimation of the direct irradiance.
For ozone the climatological values from the standard atmosphere are used (Krämer et al., 2003).

All these external input parameters to the clear sky surface radiation algorithms are temporally and spatially interpolated to the satellite observations and used on the gnu-MAGIC algorithm to derive the clear sky direct and total surface radiation for every satellite measurement and each satellite pixel.

5   Solar surface radiation (SIS / DNI)

To derive the surface solar radiation under all-sky conditions, the clear sky information as derived from the gnu-MAGIC algorithm (see Section 4) is combined with the information from the effective cloud albedo (see Section 3) using the formulas presented in Section 3.7. Figure 5-1 presents a schematic overview of the retrieval concept and the algorithm.
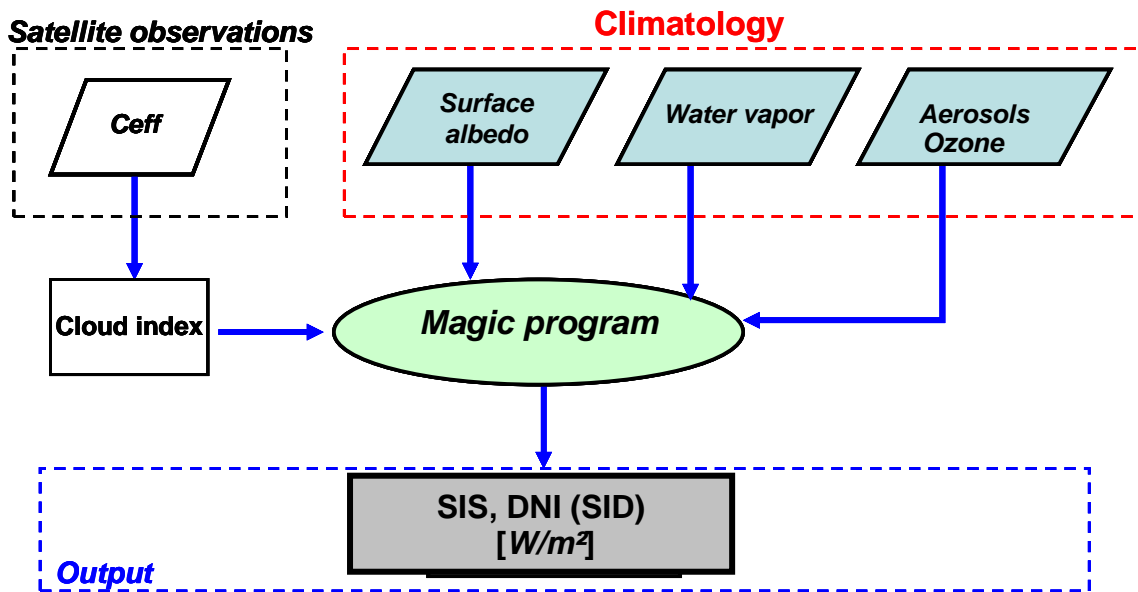
Figure 5-1: Diagram of the interface of gnu-MAGIC to the atmospheric input and the satellite observations, *Ceff* stands for the dark offset corrected and normalised Counts.

5.1   Calculation of the clear sky index and the surface radiation

The all-sky surface solar irradiance is related to the clear sky surface radiation via the clear sky index, k:

$$SIS = k \cdot SIS_{CLS} \qquad \textbf{(Equation 5-1)}$$

Here SIS_{CLS} is the solar irradiance for cloud free skies as derived from gnu-MAGIC. The direct solar radiation, SID, is derived from the clear sky index using the following formula (see also Section 3.9):

$$SID_{allsky} = SID_{CLS}\left(k - 0.38 \cdot (1-k)\right)^{2.5} \qquad \textbf{(Equation 5-2)}$$

According to Equation 3.7, for values of the cloud albedo above 0.6 the direct irradiance is zero, which is in line with observations (Skartveit et al., 1998). The direct nomalized irradiance, DNI, is derived from SID by normalisation with the cosine of the solar zenith angle (SZA):

$$DNI = SID / \cos(SZA) \qquad \textbf{(Equation 5-3)}$$

As presented in Section 3.9, the relation between the effective cloud albedo CAL and the clear sky index is mainly given by:

$$k = 1 - CAL \qquad \textbf{(Equation 5-4)}$$

Above a CAL value of 0.8 empirical corrections are needed in order to consider:
- The effect of statistical noise, which could lead to CAL values above 1 and below 0 (occurs very seldom, however have to be considered).
- The effect of saturation occurring in optically thick clouds

Equation 5-5 provides the complete k-CAL relation for all possible values of CAL. The root-mean-square deviation (RMSD) of the empirical fit is 0.1.

$$
\begin{aligned}
CAL < -0.2 &: k = 1.2, \\
-0.2 \leq CAL \leq\ 0.8 &: k = 1 - CAL, \\
0.8 < CAL \leq\ 1.1 &: k = 2.0667 - 3.6667 \cdot CAL + 1.6667 \cdot CAL^2, \\
CAL >\ 1.1 &: k = 0.05
\end{aligned}
$$
(Equation 5-5)

5.2 Averaging

Daily averages of the surface solar radiation are calculated from the instantaneous derived surface radiation data following the method published in Diekmann et al., 1988:

$$
SIS_{DA} = SIS_{CLSDA} \frac{\sum\limits_{i=1}^{n} SIS_i}{\sum\limits_{i=1}^{n} SIS_{CLS\,i}}
$$
(Equation 5-6)

SIS_{DA} is the daily average of SIS. SIS_{CLSDA} is the daily averaged clear sky SIS, SIS_i the calculated SIS for satellite image i and SIS_{CLS_i} the corresponding calculated clear sky SIS.
The number of images available during a day is denoted by n.
The larger the number of available images per day, the better the daily cycle of cloud coverage can be resolved, increasing the accuracy of the daily average of SIS. Please note that the diurnal cycle of the solar zenith angle is implicitly accounted for by using the clear sky daily mean SIS value in the averaging.
A minimum number of three available pixels per day is required to derive the daily mean for this specific pixel. The monthly average is calculated from the daily means of this month on pixel basis as arithmetic mean with a required number of ten existing daily means.
The hourly means are derived as arithmetic average from 3 observational slots, e.g., 1200 is the average of the 12:00, the 12:30 and the 13:00 slot (all times are the start time of the scan). This guarantees a higher stability in the hourly means in case of missing slots. To ensure consistent averaging and prevent double counting each full hour slot is weighted only with 25 % in the averaging (i. e., SIShm(1200) = 0.25 SIS(1200) + 0.5 SIS(1230) + 0.25 SIS(1300)). The weights are calculated for each pixel according to the respective scanning time.

The conversion from the irregular satellite projection to the regular 0.05 x 0.05 degree lon-lat-grid is conducted with the gnu-MAGIC gridding tool based on a nearest-neighbour method.

The spatial and temporal averaging of the direct normalized surface solar radiation, DNI, are conducted identical as for the surface solar irradiance, SIS, and not repeated here.

5.3 Sensitivity and dependence on input parameters of SIS / DNI

The sensitivity of the surface solar radiation on the input parameters is discussed. The section provides the uncertainty or sensitivity of SIS in relation to the input parameters. The error and accuracy of SIS is assessed by comparison with in-situ data and provided in the validation report. Beside the clear sky index, which is derived from satellite observations, aerosol and water vapour have a significant effect on the attenuation of the solar irradiance as well, while the impact of the surface albedo on the downwelling solar radiation is rather weak. A full uncertainty assessment can be found in RD.1, here we only summarize the main results.

5.3.1 Water vapor

The sensitivity of the solar surface radiation on the integrated water vapour is higher for low water vapour amounts and low solar zenith angles. The total surface irradiance shows a stronger sensitivity to uncertainties in the integrated water vapour than the direct solar radiation. Overall uncertainties in the integrated water vapour of about 1 to 2 mm translate to uncertainties of approx. 3 W/m^2, with slightly larger values under low water vapour conditions, and less uncertainties under high water vapour levels.

5.3.2 Ozone

The sensitivity of the solar surface radiation on the integrated ozone amount is in the order of 1 W/m² for typical ozone variation within the SEVIRI disk. Again the sensitivity of the solar irradiance on ozone is slightly higher than that given for the direct irradiance.

5.3.3 Aerosols

The sensitivity of the surface solar radiation to uncertainties in aerosol information is mainly governed by the aerosol optical depth. While the sensitivity of the direct irradiance by aerosols is completely governed by the AOD, the total surface solar radiation is also sensitive to uncertainties in the aerosol type, expressed by the single scattering albedo and the asymmetry parameter. In all cases, the sensitivity does also depend on the solar zenith angle.

The sensitivity on uncertainties in the AOD is much higher for the direct irradiance than for the global irradiance. Typical uncertainties in the monthly mean aerosol optical depth of 0.1 relative to a background of AOD = 0.2 leads to uncertainties in SIS of about 10 W/m^2 for a solar zenith angle of 60 degree and about 20 W/m^2 for solar zenith angle of 0 degree, both for cloudless sky (values are approx. three times higher for SID). However, for cloudy conditions these uncertainties reduce significantly with increasing cloud optical depth.

For the total surface solar radiation, additional uncertainties result from the assumptions on the aerosol optical properties, which can be in the same order of magnitude. Uncertain aerosol information is one of the major sources of the errors in the retrieval of surface solar radiation from satellite on short time scales. On the daily and monthly time scales, however, the aerosol impacts are substantially reduced compared to the instantaneous values. Further details are given in RD.1.

5.3.4 Surface albedo

The sensitivity of clear sky SIS on uncertainties and errors in the surface albedo is comparably small. Deviations of +/- 0.1 in the surface albedo lead to deviations in clear sky SIS of +/- %. The effect is almost linear. Errors in the surface albedo are expected to be typically less than 0.1, with exception of snow covered surfaces, where higher errors might occur. The effect is pre-dominantly independent on the clear sky atmospheric state.

5.3.5 Clear sky index

The clear sky index is calculated from the effective cloud albedo using Equation 5-5. For CAL > 0.8 the clouds are optically rather thick and the uncertainty in the solar irradiance is

small in absolute terms. Therefore, we focus on the region between 0 and 0.8. Here any uncertainty in the effective cloud albedo leads to identical uncertainty in the clear sky index. Thus, we are only interested in the uncertainty arising from the cloud index. Therefore, we assume a perfect clear sky irradiance.

As a result of the definition of the clear sky index an uncertainty of x % translates directly in the identical relative uncertainty for the solar irradiance, meaning a 3 % uncertainty in the effective cloud albedo leads to a 3 % uncertainty in the solar irradiance.

For the direct surface solar radiation, the sensitivity on the clear sky index is larger. An uncertainty of 2 % for the clear sky index results in an uncertainty of about 10 % in the direct irradiance, demonstrating the importance of an accurate clear sky index on the direct irradiance. Further information can be found in RD.1.

5.4 Assumption, limitations and future improvements

- The high clear sky reflection over bright surfaces (e. g., desert regions) reduces the contrast between clear sky reflection and cloudy-sky reflection. This leads to higher uncertainties in CAL and errors in the calculation of SIS and DNI over bright surfaces. The modified approach for the clear sky reflection improves the accuracy of SIS over bright surfaces, but the accuracy is still significantly lower than for other surfaces.

- In regions with long-lasting cloud cover the modified approach for the clear sky reflection overestimates the clear sky reflection. This results in an underestimation of the effective cloud albedo and an overestimation of the solar surface radiation.

- The accuracy of aerosol information is unknown in several regions of the world due to missing ground measurements. Any uncertainty in the aerosol information affects the accuracy of the surface solar radiation (in particular for the direct solar radiation), especially in regions that are dominated by cloudless sky.

- The quality of the direct irradiance strongly depends on the quality of the information about the atmospheric state, especially the aerosol information, the integrated water vapour and the clear sky index.

- The gnu-MAGIC clear sky model does currently not consider topography for the clear sky surface radiation calculations. Reduced amounts of integrated water vapour and aerosol optical depth are, however, considered in the input parameters. Only the effect of modified Rayleigh scattering is not accounted for, which is considered to be small.

Accounting for the spatial variability of clouds in Equation 5.5 has the potential to improve the accuracy of the product. This could be achieved by empirical adjustment of Equation 5 5 using the spatial variance of a 15x15 km domain as measure for the spatial variability (inhomogeneity) of clouds.

6 Improvements relative to the released MVIRI CDR

The improvements of the algorithm and input data relative to RD.1 are discussed in detail in section 3.4, 3.5, 4.4

The length of the data record will be substantially extended compared to the available CM SAF MVIRI CDR.

Special care has been taken in order to improve the homogeneity of the CDR. The available CM SAF MVIRI CDR exhibits some breaks and inhomogeneities in Europe before 1994 (Sanchez-Lorenzo et al., 2013). There are also indications of artificial shifts in the data record in other regions (Brinckmann et al., 2013). Corrupted raw data are, at last partly, the source of these breaks and inhomogeneities. Due to problems with data transmission only every second line of the broadband visible channel had been transmitted during night and twilight hours. This has been considered within the processing of the first CM SAF MVIRI only data record (RD.1), according to the EUMETSAT documentation. However, much more hours and time periods are affected. For these times the lines have been incorrectly interpreted as defined due to a missing no-data value in the raw images. More over, many other images are corrupted without being documented or listed as such. The CM SAF team performed a visual inspection of the images in order to detect all corrupted or incomplete images. This visual inspection is very time consuming, but the only possibility to avoid the use of corrupted or incomplete images. Some flaws as missing or black lines can be treated by interpolation (see section 3.5) or by assigning non-defined values. However, many corrupted images can not be used and have to be disregarded within the reprocessing in order to avoid corruption of the retrieved solar surface irradiance.

The transition between MFG and MSG is a source for serious breaks and inhomogeneities due to the change in the spectral observations from the MVIRI to the SEVIRI instruments. Respective issues have been investigated and resolved (Posselt et al. 2011; 2013). For the generation of the current SARAH data set an artificial visible broadband channel has been generated and used (section 3.5).

The IDL interpolation routine leads to circle structures in the images and has been replaced by an algorithm of R. Müller, developed within gnu-MAGIC.

A bug in the routine for the calculation of the pixel scanning time has been fixed.

7   References

Beyer H. G., Costanzo C. and Heinemann, D., 1996: Modifications of the Heliosat procedure for irradiance estimates from satellite images, *Solar Energy*, **56**, 207-212.

Bellouin, N., Quaas, J., Morcrette, and J.-J., Boucher, O., 2013: Estimates of aerosol radiative forcing from the MACC re-analysis, *Atmos. Chem. Phys.*, **13**, 2045-2062.

Benedetti, A., Morcrette, J.-J., Boucher, O., Dethof, A., Engelen, R.J., Fisher, M., Flentje, H., Huneeus, N., Jones, L., Kaiser, J.W., Kinne, S., Mangold, A., Razinger, M., Simmons, A.J. and Suttie, M., 2009: Aerosol analysis and forecast in the European Centre for Medium-Range Weather Forecasts Integrated Forecast System: 2. Data assimilation, *J. Geophys. Res.*, **114**, D13205

Brinckmann S, Trentmann J and Ahrens B., 2014: Homogeneity Analysis of the CM SAF Surface Solar Irradiance Dataset Derived from Geostationary Satellite Observations. *Remote Sensing*, **6**(1):352-378.

Cano D., Monget J. M., Albuisson M., Guillard H., Regas N., and Wald, L. A, 1986: Method for the determination of the global solar-radiation from meteorological satellite data, *Solar Energy*, **37**, 31-39.

Cros, S.; Albuisson, M. and Wald, L., 2006: Simulating Meteosat-7 broadband radiances using two visible channels of Meteosat-8. *Solar Energy*, **80**, 361–367.

Dagestad, K.-F., 2004: Mean bias deviation of the Heliosat algorithm for varying cloud properties and sun-ground-satellite geometry, *Theor. Appl. Climatol.*, **79**, 215–224, DOI 10.1007/s00704-004-0072-5

Dee, D., et al., 2011: The ERA-Interim reanalysis: configuration and performance of the data assimilation system, *Q. J. R. Meteorol. Soc.*, **137**: 553–597,

Diekmann, F.J., S. Happ, M. Rieland, W. Benesch, G. Czeplak and F. Kasten, 1988: An operational estimate of global solar irradiance at ground level from METEOSAT data: results from 1985 to 1987, *Meteorol. Rdsch.*, **41**, 65-79.

Dürr B., and Zelenka A., 2009: Deriving surface global irradiance over the alpine region from Meteosat second generation data by supplementing the Heliosat method, *International Journal of Remote Sensing*, 5821-5841, DOI 10.1080/01431160902744829.

Hammer A., Heinemann D., Hoyer C., Kuhlemann R., Lorenz E., Müller R., and Beyer H. G., 2003: Solar energy assessment using remote sensing technologies*, Remote Sens. Environ.*, **86**, 423--432.

Hammer, A., 2000: Anwendungsspezifische Solarstrahlungsinformationen aus Meteosat-Daten. Phd, School of Mathematics and Natural Sciences, University of Oldenburg.

Hess, M.; P. Köpke and I. Schult, 1998: Optical Properties of Aerosols and Clouds: The Software Package OPAC. *Bull. Amer. Meteor. Soc.*, **79**, 831-844.

Kinne, S., Schulz M., Textor C. et al., 2006: An AeroCom initial assessment – optical properties in aerosol component modules of global models, *Atmos. Chem. Phys.*, **6**, 1815-1834.

Krämer, M., Ri. Müller, H. Bovensmann, J. Burrows, J.-U. Grooß, D. S. McKenna, Ro. Müller, Th. Woyke, J. Brinkmann, E.P. Röth, R. Ruhnke, G. Günther, J. Hendricks, E. Lippert, K. S. Carslaw, Th. Peter, A. Zieger, Ch. Brühl, B. Steil and R. Lehmann, 2003: 'Intercomparison of Numerical Stratospheric Chemistry Models under Polar Vortex Conditions. *Journal of Atmospheric Chemistry*, **45**, 51-77.

Köpke P.; Hess M.; Schult I. and Shettle E., 1887: Global aerosol data set. *Tech. Rep.,* **243**, MPI Meteorology, Hamburg.

Mayer B. and A. Kylling, 2005: Technical note: "The libRadtran software package for radiative transfer calculations - description and examples of use." *Atmos. Chem. Phys.*, **5**, 1855-1877.

Meyer, R., Hoyer, C., Schillings, C., Trieb, F., Diedrich, E. and Schroedter M., 2003: SOLEMI: A New Satellite-Based Service for High-Resolution and Precision Solar Radiation Data for Europe, Africa and Asia published in *ISES Solar World Congress.*

Morcrette, J. J., Boucher, O., Jones, L., Salmond, D., Bechtold, P., Beljaars, A., Benedetti, A., Bonet, A., Kaiser, J. W., Razinger, M., Schulz, M., Serrar, S., Simmons, A. J., Sofiev, M., Suttie, M., Tompkins, A. M. and Untch, A., 2009: Aerosol analysis and forecast in the European Centre for Medium-Range Weather Forecasts Integrated Forecast System: Forward modelling, *J. Geophys. Res.*, **114**, D06206.

Müller, R.W. et al., 2003: Report of the HELIOSAT-3 software package for solar irradiance retrieval, all sky working version" *EU report of the Heliosat-3 project (http://www.uni-oldenburg.de/physik/forschung/ehf/energiemeteorologie/forschung/abgeschlossene-projekte/heliosat-3/), NNE5-2000-00413*

Mueller, R.W., K.F. Dagestad, P. Ineichen, M. Schroedter-Homscheidt, S. Cros, D. Dumortier, R., Kuhlemann R. ; Olseth J.A.; Piernavieja G.; Reise C.; Wald L. and Heinemann D., 2004: Rethinking satellite based solar irradiance modelling – The SOLIS clear sky module", *Rem. Sens. Envir.*, **91**, 160-174.

Mueller, R.W., Matsoukas, C. Behr, H.D., Gratzki and A. Hollmann, R., 2009: MAGIC - The CM-SAF operational scheme for the satellite based retrieval of solar surface irradiance - a LUT based eigenvector hybrid approach. *Remote Sensing of Environment*, **113**, 1012-1024.

Mueller, R.; Behrendt, T.; Hammer, A. and Kemper, A, 2012: A New Algorithm for the Satellite-Based Retrieval of Solar Surface Irradiance in Spectral Bands. *Remote Sens.*, *4*, 622-647.

Mueller, R and Träger-Chatterjee, C., 2014: Brief accuracy assessment of aerosol climatologies for the retrieval of solar surface radiation, *Atmosphere*, **5**, 959-972.

Perez, R., Seals, R. and Zelenka, A., 1998: Production of Site/Time-specific Hourly Irradiances -Satellite Remote Sensing vs. Network Interpolation, in Production of Site/Time-specific Irradiances from Satellite and Ground Data, *published by New York State Energy Research and Development Authority*, Report **98**-3.

Perez, R. et al., 2001: Solar resource assessment: A review, in Solar Energy - The state of the art, published by James & James Science Publishers, 497-562.

Posselt R, Mueller R, Stöckli R and Trentmann J. 2011: Spatial and Temporal Homogeneity of Solar Surface Irradiance across Satellite Generations. *Remote Sensing.*; **3**(5):1029-1046.

Posselt R., Müller, R.W., Stöckli R. and Trentmann, J., 2012: Remote sensing of solar surface radiation for climate monitoring - the CM-SAF retrieval in international comparison, *Remote Sens. Environ.,* **118**, 186-198, doi: 10.1016/j.rse.2011.11.

Posselt, R., Mueller R., Trentmann J., Stoeckli R. and Liniger M., 2014: A surface radiation climatology across two Meteosat satellite generations, Remote Sensing of Environment, **142,** 103-110.

Rigollier C., Lefevre M., Blanc P., and Wald L., 2002: The operational calibration of images taken in the visible channel of the meteosat series of satellites, *J. Atmos. Ocean. Technol.*, **19**, 1285-1293.

Rigollier C., Lefevre M., and Wald L., 2004: The method Heliosat-2 for deriving shortwave solar radiation from satellite images, *Solar Energy*, **77**, 159–169.

Sanchez-Lorenzo, A., Wild, A.M. and Trentmann, J., 2013. Validation and stability assessment of the monthly mean CM SAF surface solar radiation dataset over Europe against a homogenized surface dataset (1983–2005), Remote Sens. Environ., **134**, 355-366, doi: 10.1016/j.rse.2011.11. doi: 10.1016/ j.rse.2013.03.012

Skartveit A., Olseth J. and Tuft M., 1998: An hourly diffuse fraction model with correction for variability and surface albedo. *Solar Energy*, **63**, 173–183.

Wald, L. et al., 2002: SoDa: A project for the integration and exploitation of networked solar radiation databases, in Environmental Communication in the Information Society, *Published by the International Society for Environmental Protection*, Vienna, Austria, Editors: Pillmann and Tochtermann, 713-720.

Zelenka, A., R. Perez, R. Seals and D. Renne, 1999: Effective Accuracy of Satellite-Derived Hourly Irradiances, *Theor. Appl. Climatol.*, **62**, 199 – 207.

8 Glossary – List of Acronyms in alphabetical order

AC :   Anomaly Correlation
AVHRR :   Advanced Very High Resolution Radiometer
AOD :   Aerosol Optical Depth
CAL :   Effective cloud albedo
CDR :   Climate Data Record
CM SAF :   SAF on Climate Monitoring
COT :   Cloud optical depth
DWD :   Deutscher Wetterdienst (german meteorological service)
DNI :   Direct Normal Irradiance
ECV :   Essential Climate Variable
ECMWF :   European Centre for Medium Range Weather Forecasts
EUMETSAT : European Organisation for the Exploitation of Meteorological Satellites
FCDR :   Fundamental Climate Data Record
FMI :   Finnish Meteorological Institute
GADS/OPAC: Global Aerosol Data Set / Optical Properties of Aerosols and Clouds
GCOS :   Global Climate Observing System
GERB :   Geostationary Earth Radiation Experiment
GMS :   Geostationary Meteorological Satellite
GOES :   Geostationary Operational Environmental Satellite
k :   Clear sky index
KNMI :   Royal Meteorological Institute of the Netherlands
LUT :   Look-up table
LW :   Longwave
MACC :   Monitoring Atmospheric Composition and Climate
MAD :   Mean Absolute Difference
MAGIC :   Mesoscale Atmospheric Global Irradiance Code
MeteoSwiss : Meteorological Service of Switzerland
MFG :   Meteosat First Generation
MVIRI :   Meteosat Visible-InfraRed Imager
MSG :   Meteosat Second Generation
NOAA :   National Oceanic and Atmospheric Administration
NCEP :   National Centers for Environmental Prediction
NMHS :   National Meteorological and Hydrological Service
NWC SAF :   SAF on support to Nowcasting and Very Short-Range Forecasting (VSRF)
RMIB :   Royal Meteorological Institute of Belgium
RMSD :   Root-Mean-Square Deviation
RTM :   Radiative Transfer Model
SAF :   Satellite Application Facility
SARAH :   Surface Solar Radiation Data record – Heliosat
SD :   Standard Deviation
SEVIRI :   Spinning Enhanced Visible and Infrared Imager
SID :   Surface Direct Irradiance (beam)
SIS :   Solar Surface Irradiance
SMHI :   Swedish Meteorological and Hydrological Institute
SSA :   Single Scattering Albedo
SW :   Shortwave
SZA :   Sun Zenith Angle
UK MetOffice: Meteorological Service of the United Kingdom
WCRP :   World Climate Research Programme
WMO :   World Meteorological Organization

9   APPENDIX: Accuracies achieved for the MVIRI CDR – version 1

Statistics for the comparison of monthly mean SID between the mean of all BSRN stations and CM SAF

SIS	N_{mon}	Bias [W/m^2]	MAD [W/m^2]	SD [W/m^2]	AC	Frac$_{mon}$ > 15 W/m^2 [%]
	878	4.24	7.76	8.23	0.89	10.71

SID	N_{mon}	Bias [W/m^2]	MAD [W/m^2]	SD [W/m^2]	AC	Frac$_{mon}$ > 20 W/m^2 [%]
	805	0.89	11.0	15.67	0.83	15.4

BIAS:
The bias or (also called mean error) is simply the mean difference between the average of two datasets, resulting from the arithmetic mean of the difference over the members of the data records. It indicates whether the dataset on average over- or underestimates the reference dataset.

$$\text{Bias} = \frac{1}{n}\sum_{k=1}^{n}(y_k - o_k) = \bar{y} - \bar{o}$$

MEAN ABSOULETE DIFFERENCE (MAD):
In contrast to the bias, the mean absolute difference (MAD) is the arithmetic average of the absolute values of the differences between each member (all pairs) of the time series. It is therefore a good measure for the mean "error" of a dataset.

$$\text{MAD} = \frac{1}{n}\sum_{k=1}^{n}|y_k - o_k|$$

STANDARD DEVIATION (SD)
The standard deviation SD is a measure for the spread around the mean value of the distribution formed by the differences between the generated and the reference dataset.

$$\text{SD} = \sqrt{\frac{1}{n-1}\sum_{k=1}^{n}\left((y_k - o_k) - (\bar{y} - \bar{o})\right)^2}$$

ANOMALY CORRELATION (AC):
The anomaly correlation AC describes to which extend the anomalies of the two considered time series correspond to each other without the influence of a possibly existing bias. The correlation of anomalies retrieved from satellite data and derived from surface measurements allows the estimation of the potential to determine anomalies from satellite observations.

$$AC = \frac{\sum_{k=1}^{n}(y_k - \bar{y})(o_k - \bar{o})}{\sqrt{\sum_{k=1}^{n}(y_k - \bar{y})^2}\sqrt{\sum_{k=1}^{n}(o_k - \bar{o})^2}}$$

27

Here, for each station the mean annual cycle ȳ and ō were derived separately from the satellite and surface data, respectively. The monthly / daily anomalies were then calculated using the corresponding mean annual cycle as the reference.

FRACTION of time steps above the validation target values
A measure for the uncertainty of the derived dataset is the fraction of the time steps that are outside the requested target value'T'. The target values is given by the target accuracy of the respective CM SAF product, plus the non-systematic error (uncertainty) of the BSRN measurements (Ohmura et al. 1998).

$$\text{Frac} = 100 \cdot \frac{\sum_{k=1}^{n} f_k}{n} \quad \text{with} \begin{cases} f_k = 1 & \text{if } y_k > T \\ f_k = 0 & \text{otherwise} \end{cases}$$